

© 2018 American Meteorological Society. For information regarding reuse of this content and general copyright information, consult the [AMS Copyright Policy \(www.ametsoc.org/PUBSReuseLicenses\)](https://www.ametsoc.org/PUBSReuseLicenses).

# Whither the 100th Meridian? The Once and Future Physical and Human Geography of America's Arid–Humid Divide. Part I: The Story So Far

**Richard Seager<sup>a</sup>**

Lamont–Doherty Earth Observatory of Columbia University, Palisades, New York

**Nathan Lis**

Department of Meteorology and Atmospheric Science, The Pennsylvania State University, University Park, Pennsylvania

**Jamie Feldman**

School of Engineering and Applied Sciences, Columbia University, Palisades, New York

**Mingfang Ting, A. Park Williams, Jennifer Nakamura, Haibo Liu, and Naomi Henderson**

Lamont–Doherty Earth Observatory of Columbia University, Palisades, New York

Received 18 May 2017; in final form 8 December 2017

---

<sup>a</sup>Corresponding author: Richard Seager, [seager@ldeo.columbia.edu](mailto:seager@ldeo.columbia.edu)

**ABSTRACT:** John Wesley Powell, in the nineteenth century, introduced the notion that the 100th meridian divides the North American continent into arid western regions and humid eastern regions. This concept remains firmly fixed in the national imagination. It is reexamined in terms of climate, hydrology, vegetation, land use, settlement, and the agricultural economy. It is shown there is a stark east–west gradient in aridity roughly at the 100th meridian that is well expressed in hydroclimate, soil moisture, and “potential vegetation.” The gradient arises from atmospheric circulations and moisture transports. In winter, the arid regions west of the 100th meridian are shielded from Pacific storm-related precipitation and are too far west to benefit from Atlantic storms. In summer, the southerly flow on the western flank of the North Atlantic subtropical high has a westerly component over the western plains, bringing air from the interior southwest, but it also brings air from the Gulf of Mexico over the eastern plains, generating a west–east moisture transport and precipitation gradient. The aridity gradient is realized in soil moisture and a west-to-east transition from shortgrass to tallgrass prairie. The gradient is sharp in terms of greater fractional coverage of developed land east of the 100th meridian than to the west. Farms are fewer but larger west of the meridian, reflective of lower land productivity. Wheat and corn cultivation preferentially occur west and east of the 100th meridian, respectively. The 100th meridian is a very real arid–humid divide in the physical climate and landscape, and this has exerted a powerful influence on human settlement and agricultural development.

**KEYWORDS:** Agriculture; Climatology; Hydrometeorology; North America; Vegetation-atmosphere interactions

## 1. Introduction

John Wesley Powell was a famous explorer, scientist, ethnographer, the first person of European heritage to raft down the Colorado River as well as a longtime worker within the U.S. government. He was the second director of the Geological Survey, where he oversaw ambitious land surveys to support rational development of the West in accordance with the climatic, hydrological, and geological constraints of the land. In 1879, he prepared for Congress his “Report on the Land of the Arid Regions of the United States” (Powell 1879), which argued for the requirement of a science-based approach to the development of irrigated agriculture in the arid regions and indicated the area west of the 100th meridian, apart from the wet coastal regions, to be that area. His advice, which according to DeBuys (2001) was an early appeal to “sustainable development,” was largely ignored, and in 1890, while under assault in Congress, he published three articles in *Century Magazine* to lay out his case. In one of these articles, Powell (1890) provides his most eloquent description of the 100th meridian:

Along the hundredth meridian from Manitoba to Mexico there is a zone of semiarid land. . . . The average rainfall, which varies much from year to year, is about eighteen inches on its western margin, and increases to about twenty-four on its eastern edge. Passing from east to west across this belt a wonderful transformation is observed. On the east a luxuriant growth of grass is seen, and the gaudy flowers of the order *Compositae* make the prairie landscape beautiful. Passing westward, species after species of luxuriant grass and brilliant flowering plants disappear; the ground gradually becomes naked, with “bunch” grasses here and there; now and then a thorny

cactus is seen, and the yucca thrusts out its sharp bayonets. At the western margin of the zone the arid lands proper are reached. The winds, in their grand system of circulation from west to east, climb the western slope of the Rocky Mountains, and as they rise they are relieved of pressure and lose their specific heat, and at the same time discharge their moisture, and so the mountains are covered with snow. The winds thus dried roll down the eastern slope into lower altitudes, when the pressure increases and they are heated again. But now they are dry. Thus it is that hot, dry winds come, now and then, and here and there, to devastate the subhumid lands, searing the vegetation and parching the soil. [Powell (1890), pp 775-6]

Powell correctly notes the west–east precipitation gradient and then appears to attribute the full aridity gradient to the additional fact that the air, having crossed the Rockies, is exceedingly dry and warm, having been drained of its moisture on ascent and adiabatically warmed on descent. He correctly notes that such dry, warm air will extract moisture from the soil and vegetation. The grasslands of North America in the arid-to-semiarid plains are clearly partly a consequence of generation by the Rocky Mountains of a rain shadow to the east. Were that the only process operating, however, we would expect steady aridity east of the Rockies, so what processes allow a transformation back to humid conditions to the east of the 100th meridian?

Powell's message regarding development of the west was that the sharp gradient in aridity centered on the 100th meridian necessitated quite different policies for European settlement (farm size, crops, irrigation, water resource development, etc.) to the west and the east. This had not been music to the ears of western politicians, who disliked talk of natural environmental limits to westward expansion and did not want to wait for Powell's surveys and resource planning before advancing settlement and land use (Stegner 1954; Reisner 1986; Pisani 1992; DeBuys 2001). Nevertheless, the 100th meridian, passing through the Great Plains states of Texas, Oklahoma, Kansas, Nebraska, and the Dakotas, is a very real divide. And thanks to Powell [with assistance from his biographer, Stegner (1954)], it has been firmly etched into the nation's psychogeography: a boundary with "broad and long-standing cultural and ecological significance" (Simon 2010, p. 97). It is readily visible from space, as the user of Google Earth can quickly verify, and is also plain to window seat passengers on airplanes flying across the continent.

In his classic study of the Great Plains, Walter Prescott Webb preferred the 98th meridian as the arid–humid divide but concurred with Powell about its physical and human significance:

As one contrasts the civilization of the Great Plains with that of the eastern timberland, one sees what may be called an institutional *fault* (comparable to a geological fault) running from middle Texas to Illinois or Dakota, roughly following the ninety-eighth meridian. At this *fault* the ways of life and of living changed. Practically every institution that was carried across it was either broken and remade or else greatly altered. The ways of travel, the weapons, the method of tilling the soil, the plows and other agricultural implements, and even the laws themselves were modified. (Webb 1931, 8–9)

One pertinent example of how laws were modified in the expansion of European settlement westward is the replacement of riparian water rights with the

prior appropriation doctrine in the lands of the west (Pisani 1992). An example of how methods of development were modified is the stark reduction in density of the rail network at about the 98th meridian, which was established in the nineteenth century and persists today (see <http://www.acwr.com/economic-development/rail-maps>; last accessed 22 September 2017). As Webb (1931) points out, east of the meridian, railroads followed population, but to the west, the railroads needed to cross the plains, and this was only financially possible with investment by the national government of capital generated east of the meridian. Despite Webb, the numerical appeal of the 100th meridian being the arid–humid divide has endured. Regardless, what causes such a marked gradient in aridity across central North America, and how has it influenced the physical and human landscape? Powell (1890) provides one plausible cause of the aridity gradient. Is it correct? Will human-driven climate change transform the aridity gradient, effectively moving the 100th meridian to a new longitude? We seek to address these questions using data on climate, land hydrology, vegetation, human settlement, and the farm economy. Here, in Part I, we will address the following questions:

- (i) How is the aridity gradient realized in precipitation and soil moisture?
- (ii) Given the physical climate and land hydrology conditions, how is the aridity gradient realized in terms of natural vegetation?
- (iii) What are the climate dynamical processes that generate such a marked gradient in aridity across the 100th meridian?
- (iv) How is the aridity gradient reflected in terms of settlement and land use, area under farms, number of farms, farm size, and crops grown?

By answering these questions, we will establish a firm understanding of how planetary-scale and local physical processes in the atmosphere–land system work to establish a sharp gradient in aridity across central North America and how this gradient has fundamentally impacted the settlement of people and the agricultural economy. To our knowledge, this is the first critical examination using extensive and varied data of the realism and expression of the 100th meridian concept.

In Seager et al. (2018; hereafter Part II), we will examine how well the ensemble of climate models used in phase 5 of the Coupled Model Intercomparison Project (CMIP5) and assessed by the Intergovernmental Panel on Climate Change (IPCC) Fifth Assessment Report (AR5) simulate the aridity gradient and will use them to assess how the gradient will evolve over the coming decades as a consequence of rising greenhouse gases. We will then examine the implications for the farm economy.

## 2. Climate, land surface, environmental and agricultural data, and computation of the aridity index

### 2.1. Atmosphere and land surface hydrology data

We make use of climate and land hydrology data from the North American Land Data Assimilation System version 2 (NLDAS-2), which is based on land

surface hydrology models driven by atmospheric data (Xia et al. 2012a,b; available at <http://ldas.gsfc.nasa.gov/index.php>). Land surface models are physical models of the upper part of the land surface that solve equations for transfer of heat and moisture between the surface and the deeper layers and also contain a representation of vegetation and interactions between it, the atmosphere, and the soil below. The land surface models are forced by imposed air temperature, humidity, winds, surface radiation, and other quantities. In this case, atmospheric data from the National Centers for Environmental Prediction (NCEP) reanalysis (Kistler et al. 2001) are used in combination with precipitation data developed by the Parameter Elevation Regression on Independent Slopes Model (PRISM) Climate Group at Oregon State University [details can be found at <http://www.prism.oregonstate.edu> and in Daly et al. (2000)]. The data period covers 1979 to 2015, and the spatial resolution is  $1/8^\circ$  in latitude and longitude. The atmospheric data were used by NLDAS-2 to force three different land surface models: Mosaic, Variable Infiltration Capacity (VIC), and Noah. To assess how the aridity gradient is realized in terms of the land surface, we used the soil moisture within the top 1 m from the NLDAS-2 models. All the calculations presented were performed with all three land surface models and resulted in similar results. Here, for brevity, we only present results using the Noah model.

## 2.2. The aridity index

The aridity index (AI) for the NLDAS-2 models, denoted by subscript  $N$ , and the recent past (1979–2005), denoted by subscript  $p$ ,  $AI_{N,p}$  is computed as

$$AI_{N,p} = P_p / PET_{N,p}, \quad (1)$$

where  $P_p$  is the PRISM precipitation, and  $PET_{N,p}$  is the potential evapotranspiration computed for 1979–2015 for an NLDAS-2 model. The AI measures the amount of water delivered by the atmosphere to the land surface as a fraction of what the atmosphere could extract from a surface without water limitation. For  $AI = 1$ , these are equal, and values  $< 1$  denote degrees of aridity and values  $> 1$  humid conditions. PET is controlled by the net surface heat balance, whereby the net surface radiation (net solar radiation down minus net longwave radiation up,  $R_n$ ) has to be balanced by latent heat loss by evapotranspiration (ET) plus sensible heat loss and heat flux into the ground ( $G$ ). PET is indirectly controlled by air temperature  $T_a$ , which controls saturation specific humidity  $e_s$ , air humidity  $e_a$ , and surface wind speed (measured at 2 m above the surface)  $u_2$ , which influence the turbulent heat exchange by actual evapotranspiration ET and sensible heat flux. The vapor pressure deficit (VPD) is represented by  $e_s - e_a$ . How these atmospheric variables vary determines how the latent and sensible heat fluxes adjust to balance the net radiation plus ground heat flux. A common way to calculate this balance is the Penman–Monteith equation, which is derived by linearizing the Clausius–Clapeyron equation around the surface temperature. Here, we use the United Nations Food and Agriculture Organization version of the Penman–Monteith equation, which is developed for a well-watered grass crop (Allen et al. 1998). The derivation of the following equation for PET, which allows for aerodynamic and

stomatal resistance to evapotranspiration, can be found online [<http://www.fao.org/docrep/X0490E/x0490e06.htm#formulation%20of%20the%20penman%20monteith%20equation>; last accessed 28 August 2017; see also Allen et al. (1998)]:

$$\text{PET}_{N,p} = \frac{0.408\Delta(R_{n,p} - G) + \gamma \frac{900}{T_{a,p} + 273} u_{2,p}(e_{s,p} - e_{a,p})}{\Delta + \gamma(1 + 0.34u_{2,p})}, \quad (2)$$

where the variables on the right-hand side are taken from the NLDAS-2 land surface models and atmospheric forcing fields provided at monthly resolution.<sup>1</sup> Parameter  $\Delta$  is the slope of the vapor pressure curve with respect to temperature ( $\text{kPa } ^\circ\text{C}^{-1}$ ), and  $\gamma$  is the psychrometric constant. This version of the Penman–Monteith equation was used, for example, in global drought and climate change assessments by Dai (2011), Sheffield et al. (2012), Scheff and Frierson (2014), and Cook et al. (2014).

AI is a common means of climate classification with a long history (Transeau 1905; Budyko and Miller 1974). It is most often used in terms of a long-term mean with no reference to seasonality. However, we wish to determine physical mechanisms whereby levels of aridity are established. These will rely on the seasonal cycle of temperature and precipitation. For example, regions that have the same amount of precipitation, but focused in the cool, low ET or warm, high ET season, could have quite different levels of aridity. To examine mechanisms, we will evaluate AI at the seasonal time scale, evaluated as the seasonal mean of  $P$  divided by the seasonal mean of  $\text{PET}_{N,p}$ . To examine how the aridity gradient is established, we will examine moisture transports by the mean and transient atmospheric flow using the European Centre for Medium-Range Weather Forecasts (ECMWF) interim reanalysis (ERA-Interim) dataset for 1979 to 2015 (Dee et al. 2011). ERA-Interim is chosen because it assimilates precipitation-sensitive irradiances and is considered valuable for hydrological cycle research. We have used it to develop a “best practices” methodology for diagnostic computation of moisture budgets (Seager and Henderson 2013) and have applied it to understanding the past and future hydrological cycle over North America (Seager et al. 2014).

### 2.3. Potential vegetation, land cover, land use, and farm economy data

To examine the expression in terms of vegetation, we examined both actual land cover, which is heavily influenced by agriculture and other land use, and “potential vegetation,” which is an estimate of what would grow in any location in the absence of human intervention. We used the 2011 observed land cover dataset from the National Land Cover Database [<https://www.mrlc.gov/nlcd2011.php>; Homer et al. (2015)] and the Environmental Site Potential dataset from the LANDFIRE database (<https://www.landfire.gov/about.php>). For land use and farm economy, we examined the type of agricultural use, crops grown as percent of cropped land, and farm numbers and size using the USDA/National Agriculture Statistics Service

<sup>1</sup> Using monthly mean temperature to evaluate  $e_s$  will lead to underestimation due to the non-linearity of the Clausius–Clapeyron equation. See discussion in Seager et al. (2015).

2012 Census of Agriculture data at the county level ([www.agcensus.usda.gov/Publications/2012/Online\\_Resources/Ag\\_Census\\_Web\\_Maps/Overview](http://www.agcensus.usda.gov/Publications/2012/Online_Resources/Ag_Census_Web_Maps/Overview)). For private (non-Federal owned) rangelands, defined as grasslands that provide forage for grazing animals, we used data from the USDA Natural Resources Conservation Service (<https://www.nrcs.usda.gov/wps/portal/nrcs/detail/national/technical/nra/nri/?cid=stelprdb1253602>), which provides area in hectares that we convert to the percent of rangeland for each U.S. county.

### 3. Results

#### 3.1. Mechanisms of generation of the aridity gradient

We begin by showing in [Figure 1](#) seasonal maps of  $P$ ,  $PET_{N,p}$ , and  $AI_{N,p}$ , as well as their annual means computed as the average of the four seasonal values.

It is notable that neither  $P$  nor  $PET$  has a west–east gradient oriented across a well-defined north–south dividing line as strong as that in the  $AI$ . However, they combine to allow  $AI$  to exhibit this. Noting that  $\partial(AI)/\partial\lambda = PET^{-2}(PET\partial P/\partial\lambda - P\partial PET/\partial\lambda)$ , where  $\lambda$  is longitude, since  $\partial P/\partial\lambda$  is generally positive and  $\partial PET/\partial\lambda$  is negative across the 100th meridian, these combine to create a strong west–east gradient. During the winter half-year, there are two notable  $P$  maxima: one over the west coast, from central California to Washington, and the other over the southeastern United States. The southeastern maximum will create an east–west aridity gradient across the southern plains. In the summer half-year, there is a clear east–west  $P$  gradient, with little  $P$  west of the 100th meridian and maximum  $P$  in the eastern plains (spring) and southeastern and northern plains (summer). Throughout the year, across the plains,  $PET$  has a gradient from a maximum in the southwest (Texas) to a minimum in the midwest and northeast. Hence, both  $P$  and  $PET$  contribute to spatial gradients in  $AI$ , but it is their combination that creates the much stronger zonal than meridional gradients. In the annual mean, the marked west–east aridity gradient in the plains is clear, although a case might be made that [Webb \(1931\)](#) was correct that the 98th meridian is a better delimiter of the arid–humid divide than the more numerically convenient 100th meridian.

Next, we determine what climate variables are responsible for the west–east gradient in  $AI$ . To do this, we computed the  $AI$  after removing the zonal variations in particular climate quantities by using their zonal mean values instead. It was found that the zonal variation in net radiation  $R_n$ , temperature  $T_a$  (which also controls  $e_s$ ), and wind speed  $u_2$  contribute very little to the west–east gradient of  $AI$ . The term  $R_n$  tends to make  $AI$  slightly less in the west because dry soils increase longwave cooling and reduce the net radiation to sustain  $PET$ , but this is a response to aridity rather than a cause of it. Temperature also contributes to a slight lowering of  $AI$  in the west because of cooler values at higher elevations.

In contrast to these weak zonal variations, the zonal variation of  $VPD$  acting alone creates a vast region of higher aridity in the interior west that extends to the plains and generates a gradient of aridity across the interior United States from high in the southwest to low in the southeast ([Figure 2](#)) that contributes to the west–east aridity gradient. This would appear to be the mechanism for the aridity gradient proposed by [Powell \(1890\)](#). However, it is not created the way Powell imagined.

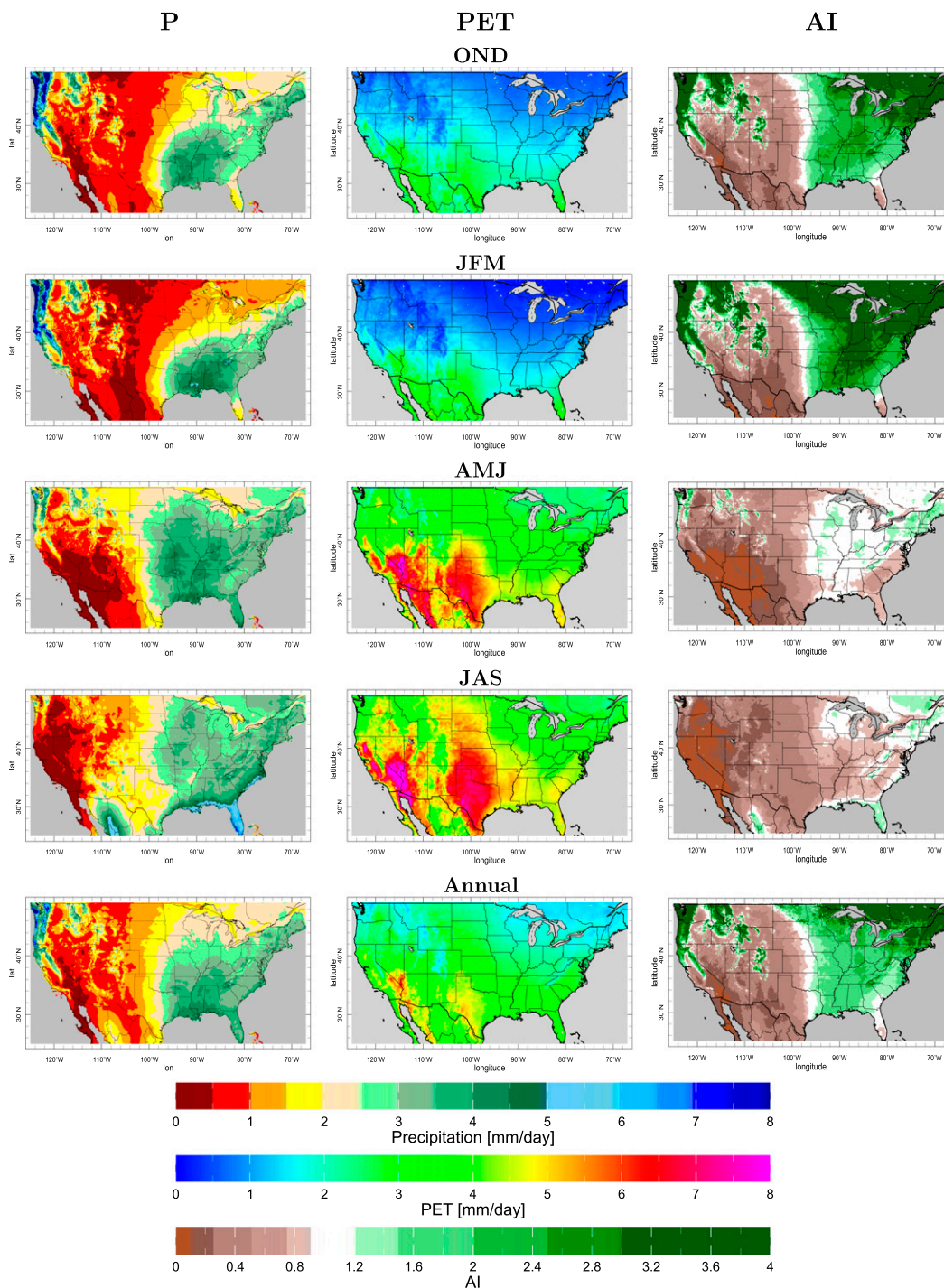
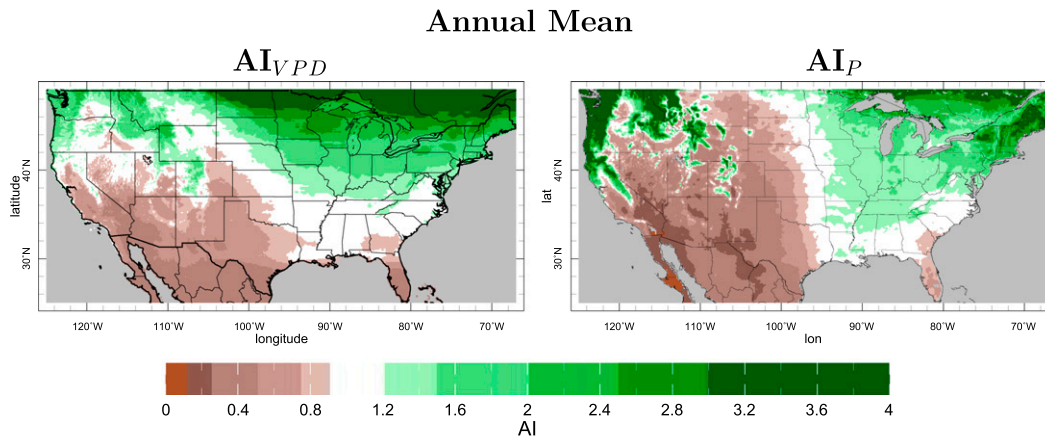


Figure 1. (left) The precipitation, (middle) potential evapotranspiration, and (right) aridity index ( $AI = P/PET$ ) as evaluated from the NLDAS-2 forcing and Noah land surface model for seasons (from top) October to December, January to March, April to June, and July to September and the annual mean (average of the four seasonal values). Units are  $\text{mm day}^{-1}$  for  $P$  and  $PET$ .



**Figure 2.** The annual mean aridity index for the case where (left) only VPD varies with longitude and (right) only precipitation varies with longitude. Latitudinal variation of all climate quantities is retained.

He thought low humidity west of the 100th meridian, derived from winds from the west descending the Rockies, dried after losing moisture from ascent, cooling, condensation, and precipitation on the windward side. Although we do not show it here, the maps of VPD in Seager et al. (2015) show that during the winter season, when the continent is most prone to westerly winds, the zonal gradient is weak. It is much stronger in spring and summer, when very high temperatures and low humidity develop in the southwest, while to the east, in spring and summer,  $e_a$  rises with  $e_s$ , keeping VPD in check.

However, it is also clear that the VPD variation mechanism does not create the north–south isolines of equal aridity that are such a striking feature of the plains. Zonal variations of  $P$ , acting alone to create zonal variations, can generate this sharp gradient (Figure 2). Hence, while the Powell mechanism is augmenting, it is the more straightforward, strong west–east gradient in  $P$  that primarily generates the west–east gradient in aridity.

### 3.2. Atmospheric circulation and the west–east precipitation gradient across the 100th meridian

Next, we turn to how atmospheric circulation and moisture transport generate the sharp west–east precipitation gradient across the 100th meridian. This requires a seasonal analysis. Figure 3 shows the vertically integrated moisture transport vectors evaluated as the seasonal average of 6-hourly data and, hence, including the effects of both the time mean flow and transient eddies overlaid over  $P$ .

In winter, the moisture transport has a strong zonal component. The wet conditions at the west coast are related to moisture coming in from the Pacific Ocean, which is effectively blocked by the Rocky Mountains, creating, in the lee, a rain-shadow effect and aridity. Alone, this would not create an aridity gradient in the middle of the continent. What does create the gradient is the southerly component

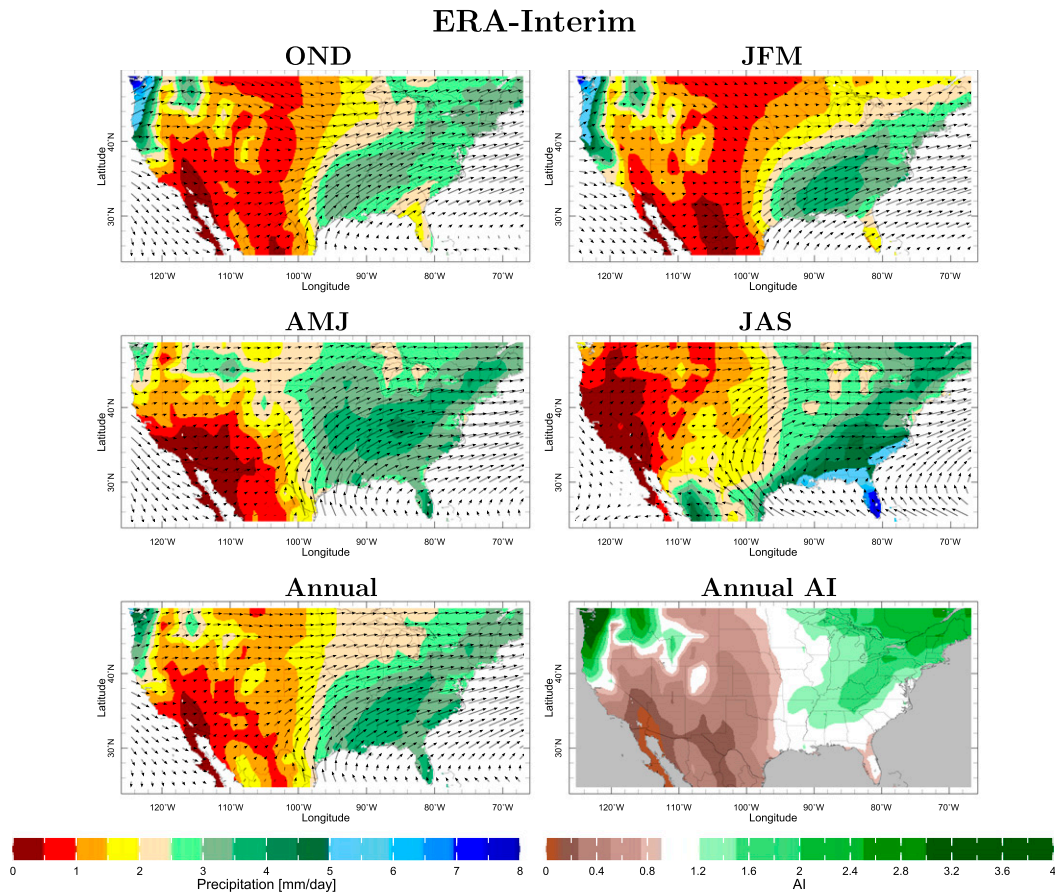


**Figure 3.** Vectors of vertically integrated moisture transport by the mean plus transient flow (arrows) and precipitation (colors) for October to December, January to March, April to June, and July to September and annual using data from ERA-Interim.

of moisture transport east of the 100th meridian. This is primarily caused by the winter season transient eddies in the beginning longitudes of the North Atlantic storm track, where storms extract moisture from the Gulf of Mexico and the western North Atlantic and converge it over the southeastern United States (Seager et al. 2014). Since in the winter season the potential and actual evapotranspiration are low (Figure 1; Seager et al. 2014), this enhanced moisture supply to the east, relative to the west of the plains, effectively generates a west–east aridity gradient.

During summer, there is strong southerly flow as part of the Great Plains low-level jet (LLJ) from the Gulf of Mexico into the Great Plains, as previously noted by Higgins et al. (1999). This brings moist air into the plains and creates the potential for precipitation. Although the moisture convergence is more widespread in winter than in summer, summer precipitation is generally greater in the plains due to the higher evapotranspiration and recycling (Seager et al. 2014). To the east of the 100th meridian, the flow is from the southeast, convergent of moisture, and the precipitation is high. To the west of the meridian, the flow is from the

southwest, divergent of moisture, and the precipitation is low. Hence, longitudinal variations in the zonal component of the flow into the plains are important in creating the summer half-year west–east aridity gradient. The southerly flow over the North American continent originates in the subtropical anticyclone–monsoon couplets argued for by [Rodwell and Hoskins \(2001\)](#) and lies on the western flank of the North Atlantic subtropical high. Precipitation and atmospheric heating forces upward motion that, to conserve vorticity, requires southerly flow. The creation of the concentrated LLJ out of this general southerly flow arises in two ways that are not mutually exclusive. First, the topography of the Sierra Madre Occidental in Mexico and the Rocky Mountains in the United States can block easterly trade wind flow and divert it north ([Rodwell and Hoskins 2001](#); [Ting and Wang 2006](#)). Second, the sloping surface of the plains responds to summertime heating with lower pressure over the mountains than to the east, generating a southerly jet ([Parish and Oolman 2010](#)).

Hence, the aridity gradient ultimately originates in planetary-scale atmospheric motions throughout the year. That said, in contrast to the featureless landscape of the Great Plains, the atmosphere above contains a rich variety of dynamic phenomena. The summer LLJ and associated northward moisture transport, convection, and precipitation are strongest at night. The nighttime peak of the LLJ arises in two ways. During the day, radiative heating of the sloping surface causes a westward pressure gradient and upslope, easterly flow that peaks around sunset. Inertial oscillation of this flow rotates it clockwise and creates a nighttime southerly jet. By the same process, cooling of the surface at night creates northerly flow during the day. Second, as boundary layer turbulence ends after daytime, frictional retardation of the LLJ weakens, and it accelerates. The nighttime precipitation peak might also be aided by eastward propagation of storms generated over the Rockies during the day. These processes are collectively examined by [Wallace \(1975\)](#), [Higgins et al. \(1999\)](#), [Jiang et al. \(2007\)](#), [Parish and Oolman \(2010\)](#), and [Riley et al. \(1987\)](#). To add complexity, the initiators of nocturnal convection include local synoptic conditions and surface boundary variations that can drive convergence ([Reif and Bluestein 2017](#)). Hence, while planetary-scale processes are an ultimate driver of the aridity gradient in the warm season, it is the coupling down to local processes at the mesoscale and below that achieves this effect.

In terms of the relative contribution of the winter and summer half-years to the aridity gradient, the precipitation over the more humid eastern plains is larger in summer than winter. This is despite more widespread moisture convergence in the winter than summer and arises from the much larger evapotranspiration in summer than winter ([Seager et al. 2014](#)).

#### 4. Expression of the 100th meridian in the natural landscape

Powell originally identified the 100th meridian in terms of the change in vegetation that occurs around this longitude. Since his time, the plains have been extensively transformed during the twentieth century by the expansion of agriculture and the replacement of natural vegetation with crops, the removal of woodlands, and the drainage of wetlands. Hence, we examine the west–east gradients in the vegetation that would occur in the absence of human action (potential

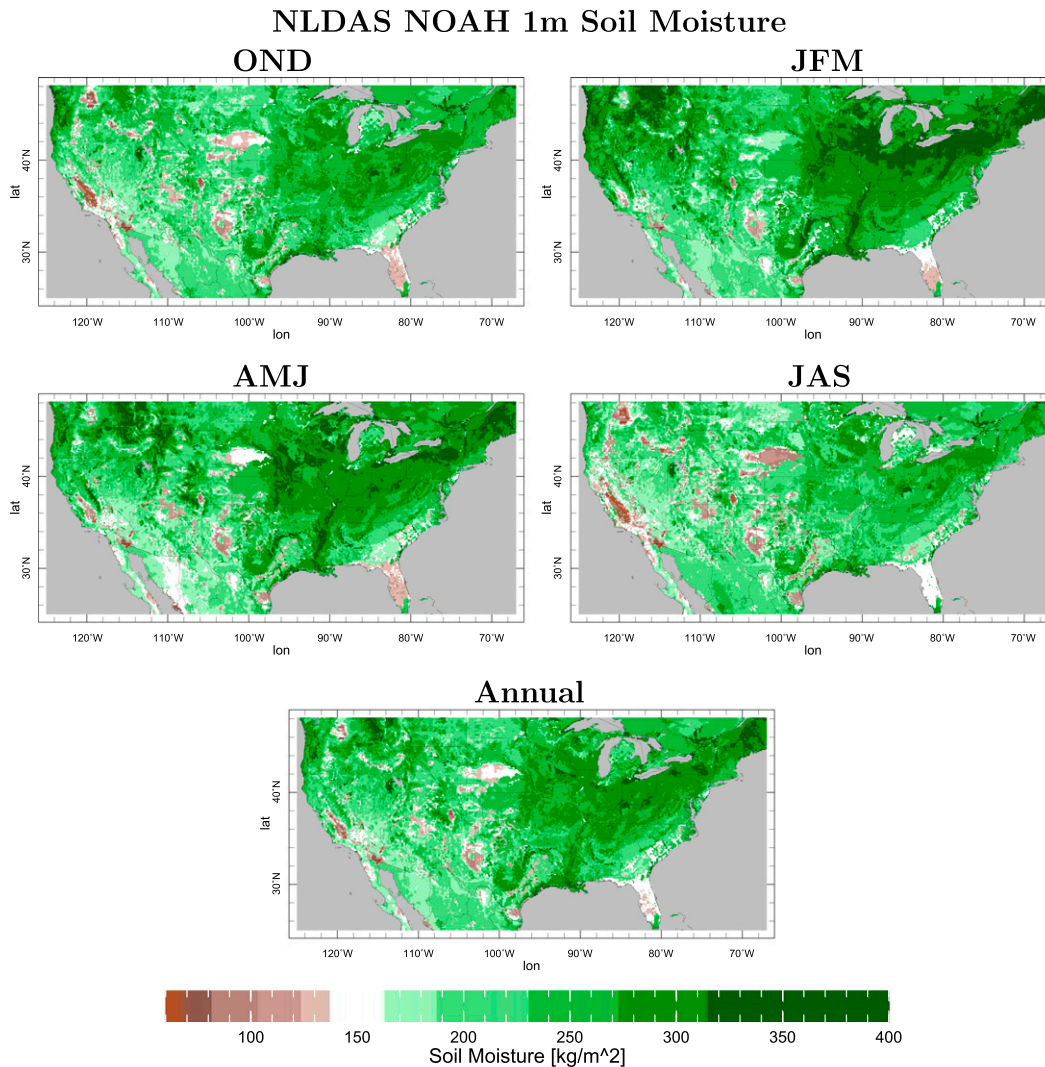


**Figure 4.** The soil moisture integrated to 1-m depth (kg) from the NLDAS-2 Noah land surface model averaged into seasonal means for October to December, January to March, April to June, and July to September.

vegetation), in the actual vegetation, and in crops. In addition, we examine if the 100th meridian is clear in soil moisture and, hence, the land hydrology that supports vegetation.

#### 4.1. Soil moisture

The 100th meridian gradient is very well expressed in terms of upper 1-m soil moisture year-round (Figure 4). Soil moisture increases with precipitation and snowmelt and decreases with evapotranspiration and surface and subsurface runoff. Hence, the fact that soil moisture clearly represents the aridity gradient indicates it

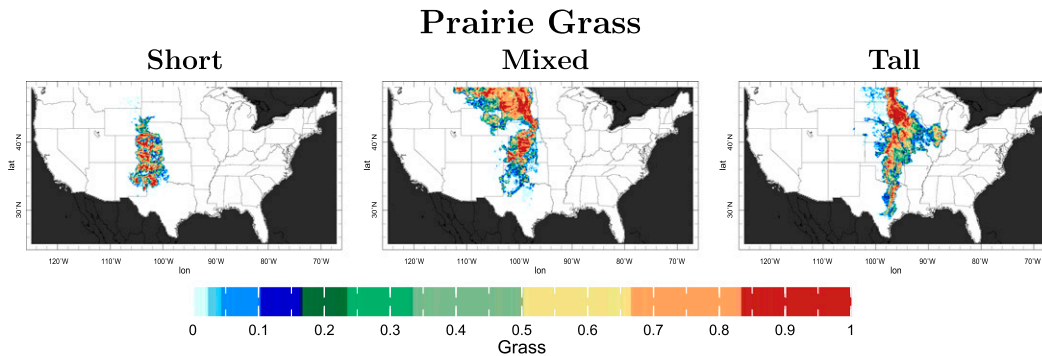


**Figure 5. Fractional land cover of potential vegetation for (left) shortgrass, (center) mixed grass, and (right) tallgrass.**

is established primarily by precipitation and secondarily by the VPD, and the spatial gradients in runoff are of less importance. The potential ET will be influenced by the gradient in VPD, but the actual ET, which influences soil moisture, likely acts as a negative feedback to offset the aridity gradient by tending to reduce soil moisture less in the arid west than in the humid east.

## 4.2. Potential vegetation

The term potential vegetation is used to describe vegetation that would be on the landscape in the absence of human interference. This is close to what Powell described in his writings from a time before massive human transformation of the plains. We are aware, however, of criticism of the concept of potential vegetation because of the difficulty of estimating a state in the absence of human interference and the reality of ecosystem dynamics and transient change (Chiarucci et al. 2010), which is certainly the case for the plains (Engle et al. 2008). However, we do consider the concept valid for our modest purpose here, which is to identify the spatial changes in grasslands across the plains. Here, we use the related “environmental site potential,” which is evaluated using “the current climate and physical environment, as well as the competitive potential of native plant species” (<http://www.landfire.gov/NationalProductDescriptions19.php>). Figure 5 shows percent land cover for three categories: shortgrass, mixed, and tallgrass prairie. The 100th meridian has a remarkable realization in the grasses that can grow in the plains, with tallgrass prairie essentially limited to the east of a north–south line that is very close to the 100th meridian, while shortgrass prairie is limited to the west. Hence, the gradients in aridity and soil moisture are sufficient to establish a quite remarkable zonal transition in the grasslands ecology.

## 5. Expression of the 100th meridian in current land cover, settlement, and agriculture

### 5.1. Land cover

Since the early twentieth century, the plains have been transformed by the introduction of agriculture and widespread growing of grains. In Figure 6, we show

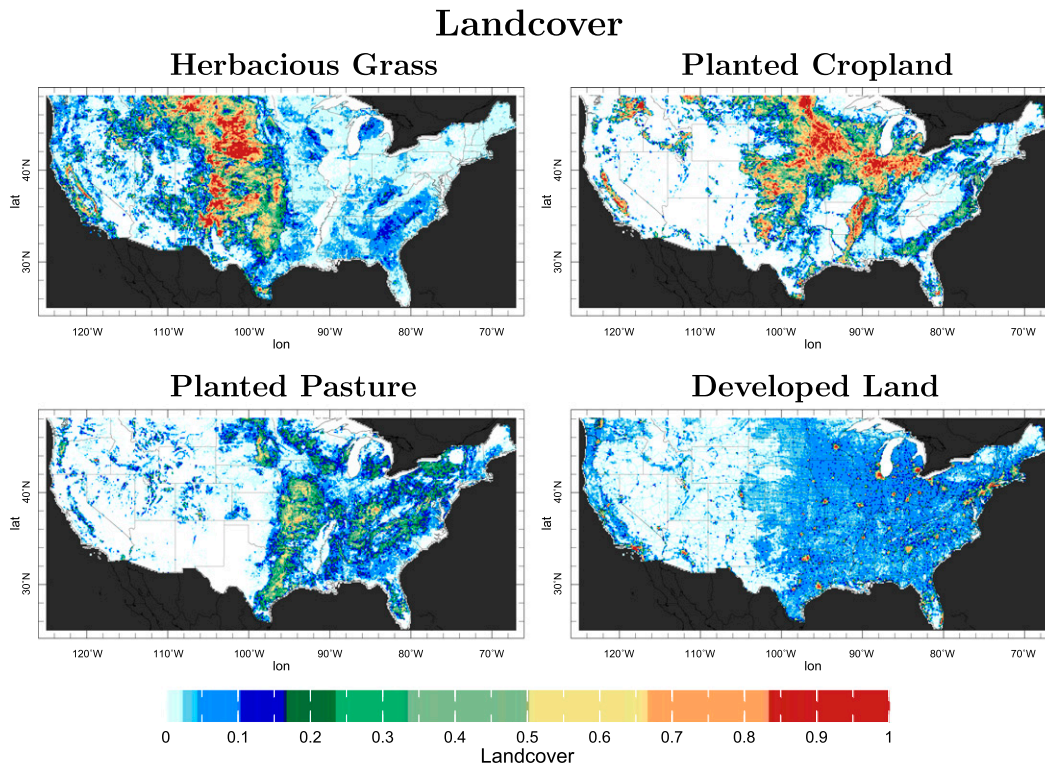


**Figure 6.** Fractional actual land cover of (top left) herbaceous grass, (top right) planted cropland, (bottom left) planted pasture, and (bottom right) human-developed land.

the fractional land cover of the two dominant categories in the plains: herbaceous grasses and planted cropland. The grasses (remaining prairie and also grazing lands) are primarily to the west of the 96th meridian, with a farther increase west of the 100th meridian. Planted cropland conforms to the 100th meridian less than the environmental site potential or other land-cover variables examined so far. The arching Corn Belt in the Midwestern states is clearly seen, but in the central and southern Great Plains, planted cropland is actually a larger percent of area in the west than the east. This is primarily because of the rough terrain of the Ouachita Mountains and the Ozark Plateau in Oklahoma, Arkansas, and Missouri. The Nebraska Sandhills, centered on 43°N, 102°W, also stand out as a longitudinal anomaly in planted cropland because the sandy soils of these stabilized sand dunes are not suitable for agricultural development. There is a clear decline in planted cropland west of the 104th meridian. Land planted for pasture (primarily hay) shows a marked east–west contrast at the 98th meridian, very little west of the 100th meridian, and a clear north–south band in the eastern plains. Figure 6 also shows the fractional coverage of developed land, which is land converted into nonagricultural use by humans, including housing, commercial and institutional use, transportation, parks, and sports facilities. This increases dramatically as the plains are crossed from west to east, making it clear that the 100th meridian is well expressed in the pattern of human settlement and population.

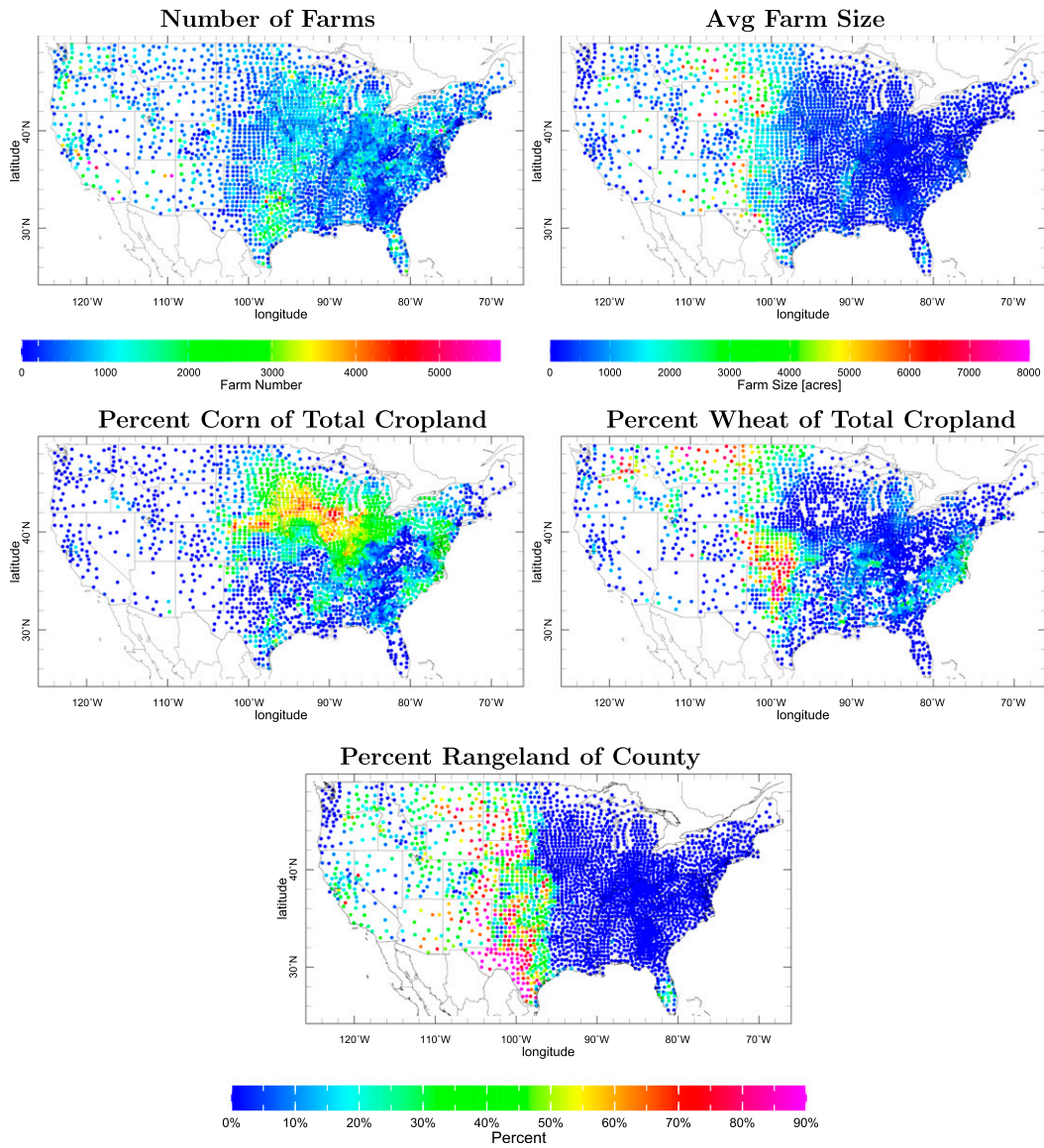


Figure 7. (top left) The number of farms, (top right) the average farm size, (bottom left) the percent of cropped land under corn, and (bottom right) the percent of cropped land under wheat for each U.S. county.

## 5.2. Agricultural economy

Although whether the land is cropped or not does not show a strong reflection of the 100th meridian, other aspects of farm economy might. In Figure 7, we show the number of farms and average farm size for each county. At all latitudes, the number of farms is at its maximum somewhere between 100° and 90°W and is uniformly low west of the 100th meridian. Consistently, farm size has a modest tendency to be larger west of the 100th meridian than in the eastern plains. A steady west–east gradient in the number of farms does not apply in the southern plains, where the maximum is around

the 98th–96th meridians, with fewer to the west, which is more arid, and to the east, which is the rough terrain of the Ouachita and Ozark ranges. Fewer but larger farms west of the 100th meridian are consistent with lower land productivity due to aridity.

The 100th meridian is also apparent in the choice of crop. [Figure 7](#) shows the percent of total cropland planted in corn and wheat in each county. Corn requires a warm and humid climate, while wheat can grow effectively in a more arid climate. The contrast is most stark in the northern plains, where up to 70% of cropland is corn east of the 100th meridian but typically much less than 20% to the west. By contrast, wheat declines from typically 40% of cropland west of the 100th meridian to less than 10% to the east. Wheat cultivation peaks at around the 100th meridian, especially in the central plains, and is typically much less than 20% to the east, where corn is favored, and to the west, where greater aridity favors rangeland. One major exception to the east–west contrast is the area of a high percentage of corn in southern Nebraska, where the Ogallala aquifer allows extensive irrigated corn cultivation. Also shown in [Figure 7](#) is the percent of each county that is rangeland. This also shows that rangeland (i.e., land that is unimproved and used for livestock forage) is concentrated in the western plains (but with the 96th meridian appearing as the divider) clearly responding to the west–east aridity gradient.

## 6. Variability and change in the aridity index over 1979 to 2015

Inevitably, as climate changes over North America due to rising greenhouse gases ([Maloney et al. 2014](#)), the AI will change. This is analyzed in [Part II](#), where we show that models project a general increase in aridity and an eastward movement of the climatically defined 100th meridian (i.e., the longitude where  $AI \approx 1$ ). In [Figure 8](#), we show longitude–time (Hovmöller) plots of the annual mean AI (computed as the average of the four seasonal values for each year) for the northern ( $42^\circ - 48^\circ\text{N}$ ), central ( $36^\circ - 42^\circ\text{N}$ ), and southern ( $30^\circ - 36^\circ\text{N}$ ) plains. These plots also show the interannual variability, making clear that the AI can vary quite substantially year to year as well as on longer multiyear-to-decadal time scales. It should be noted that the AI is conceived as a measure of mean climate and not of climate variability, but, nonetheless, this does make clear that in any one year or run of years, the level of aridity within the plains can be quite different to the longer-term average. We also show in [Figure 8](#) the Hovmöller plots for the cases where (center column)  $P$  varies but PET is held to climatological seasonal values and (right column)  $P$  is held to seasonal climatological values but PET varies. From north to south across the plains,  $P$  variability influences AI variability and dominantly so in the central and southern plains. In the northern plains, PET variability is also very important. This follows from a local maximum of temperature variability in the northern plains that arises from its remoteness from the Pacific and Atlantic Oceans and exposure to air mass incursions from both the Arctic and Gulf of Mexico. Returning to the full AI, it is notable amid the interannual variability that there are no years when the west–east aridity gradient across the plains disappears or reverses. The full AI also shows a general trend over 1979 to 2015 of increased aridity (lower values of AI) and an eastward movement of the climatically defined 100th meridian (where  $AI \approx 1$ ). In the southern plains, this has been contributed to by a  $P$  reduction, and at all latitudes, increasing PET has driven heightened aridity and eastward encroachment of aridity values.

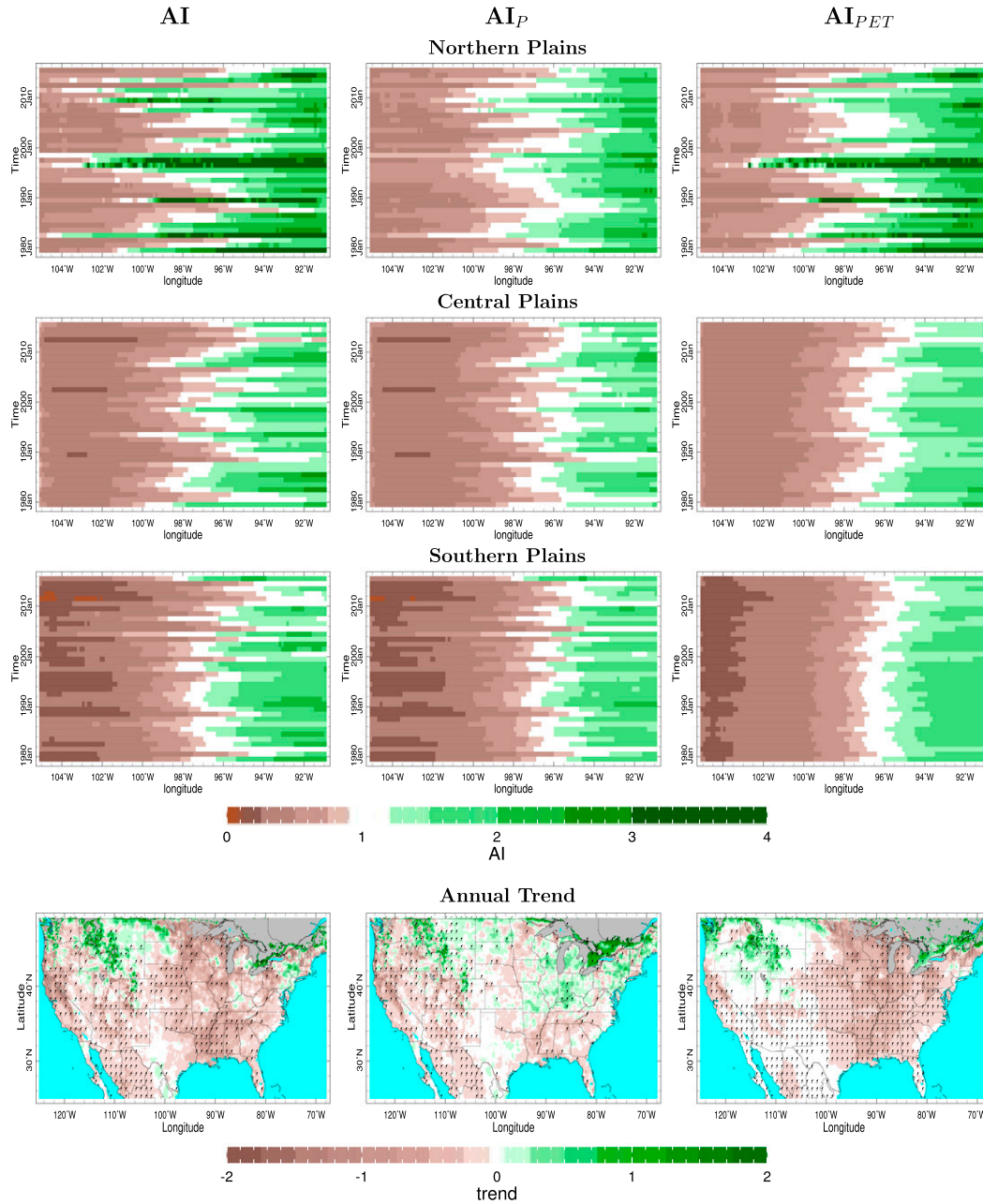


Figure 8. Time–longitude Hovmöller plots of the annual mean AI latitudinally averaged over the (top) northern, (middle) central, and (lower) southern plains for the (left) total AI, (middle) AI induced by  $P$  variability alone with fixed seasonal climatological PET, and (right) AI induced by PET variability alone with fixed seasonal climatological  $P$ . The corresponding maps of total,  $P$ -induced, and PET-induced AI trends are shown in the bottom row, with stippling indicating significance at the 10% level. The trend is defined as change in AI over the 1979 to 2015 period.

The bottom row of [Figure 8](#) shows maps of the linear trends of total AI and the *P*- and PET-induced AI. The trend since 1979 has been widespread increasing aridity, but with larger changes east of than west of the 100th meridian in the plains. Precipitation reduction has induced widespread increased aridity but with large areas of significance confined to the west. In contrast, PET has induced (via warming; not shown) statistically significant increases in aridity east of the 100th meridian. The combined effect suggests the “climatic 100th meridian” has shifted eastward amid a more general increase in aridity over the past three decades. This is consistent with the climate model projections for the aridity gradient to be presented in [Part II](#), but it should be noted that the precipitation changes over the 1979 to 2015 period are also influenced by the atmospheric teleconnection response to natural decadal variability of tropical Pacific sea surface temperatures ([Seager and Vecchi 2010](#); [Seager and Hoerling 2014](#); [Delworth et al. 2015](#)).

## 7. Discussion and conclusions

John Wesley Powell’s introduction into the national conscience of the concept of the 100th meridian as an arid–humid divide in the center of the continent of both environmental and social significance has been shown to be valid. In the 138 years after his writings, this arid–humid divide remains strongly evident in agricultural practice. In this paper, we have examined the physical causes of the divide, its reflection in the landscape, and its realization in the agricultural economy. Our conclusions are as follows.

- (i) The aridity gradient across central North America is not a simple result of the rain-shadow effect of the Rockies, which cannot explain the zonal gradient east of the Rockies. Powell’s mechanism of subsidence down the eastern slope of the Rockies of dry, warm air does indeed contribute to creating the aridity gradient. However, more fundamentally, the gradient arises from the increase in precipitation from west to east. Only during winter, when the midlatitude westerlies are dominant, does a strong rain shadow develop east of the plains. During this season, east of the 100th meridian, storm systems effectively transport moisture into the eastern plains and southeastern United States from the Gulf of Mexico and subtropical western North Atlantic. During the summer, the blocking of the easterly trade winds by the Rockies creates the Great Plains low-level jet and southerly flow across the plains. West of the 100th meridian, the flow is from the arid southwest, aided by a slight westerly orientation, but to the east, the flow is from the Gulf of Mexico, and higher precipitation results. Hence, the aridity gradient and the reality of the 100th meridian arid–humid divide arise from the rain-shadow effect and the beginning longitudes of the North Atlantic storm track in winter, and from the blocking of the trade winds by the Rockies and generation of southerly flow in the summer.
- (ii) The imposition of an aridity gradient on the North American continent by meteorological processes interacting with topography and geography is well reflected in the land surface both in terms of soil moisture and the potential vegetation that is estimated would grow in the absence of human interference, with both showing a sharp transition close to the

100th meridian. This is consistent with [Powell \(1890\)](#), who first identified the 100th meridian as a boundary by noting the stark change in vegetation across this longitude.

- (iii) Despite a century of agricultural and economic development and the transformation of natural vegetation into farmland, the 100th meridian is still clearly seen in the pattern of human settlement, in what crops are grown, and in the agricultural economy. The density of settlement and number of farms sharply decreases going west across the 100th meridian, while farm size increases. To the west of the 100th meridian, wheat is the dominant crop. Two exceptions to the 100th meridian divide are the widespread cultivation of corn west of the 100th meridian in Nebraska and pieces of neighboring states, where irrigation from the subsurface Ogallala aquifer is possible, and the lack of farms in the eastern southern plains, where the harsh topography of the Ozarks and Ouachita Mountains makes farming impossible.
- (iv) Over the past decades, aridity has increased, and there has been an eastward movement of given aridity values. This is contributed to most strongly by warming-induced increases in PET. The *P*-induced changes in AI, most notably in the west, could be related more to natural decadal variability than to human-induced climate change.

One valid question is whether the gradient across the 100th meridian in aspects of farm economy was influenced by any public or private sector policy that differed depending on whether land was west or east of the meridian. One contender might be the Newlands Reclamation Act of 1902, which led to the creation of the Bureau of Reclamation and funded irrigation projects across the west. However, the Reclamation Act eventually applied to all of the states that straddle the 100th meridian and makes no distinction between lands to the west and east of the meridian. Similarly, the prevailing system of water law tends to vary from riparian rights in the east, a system imported from Europe, to the doctrine of prior allocation in the west ([Pisani 1992](#)) but does not divide along the 100th meridian. Our own research found only one case where the 100th meridian was encoded in law, and that concerned some rather modest aspects of the USDA's Conservation Reserve Program ([Simon 2010](#)). Consequently, we consider that the gradients in social and economic structure across the plains are (to use a loaded term) "environmentally determined" and not the result of a conception of an arid-humid divide that became established in policy. West of the 100th meridian, greater aridity favors wheat and ranching over corn, and the reduced yield per acre and vulnerability to drought favors greater farm size in order to secure income ([Baltensperger 1987](#)). In the middle of the past century, drought and introduction of mechanization and crop technology combined to favor further increase in farm size in the western plains, compared to the eastern plains, where intensification of production was more feasible ([Baltensperger 1987](#)).

To conclude, large-scale meteorological processes establish the 100th meridian at the center of a strong zonal aridity gradient in the central North American continent and this gradient greatly influences land surface hydrology and vegetation and has, subsequently, impacted agricultural, economic, and social development. However, climate changes and the aridity and its gradient in the Great Plains

would have been different in the past. Grasslands in North America were well established by the middle Miocene (Strömberg 2011). There is continuing debate as to whether their origin and current composition developed in response to falling CO<sub>2</sub> (Jacobs et al. 1999) or climate change and emerging seasonal aridity (Pagani et al. 1999; Beerling and Royer 2011), but a recent analysis of changes in ocean temperatures and meridional gradients of temperature emphasizes the role of falling CO<sub>2</sub> (Herbert et al. 2016). However, the current North American grassland biome, nearly devoid of trees, appears to be of relatively recent origin. During the last glacial to early Holocene, there was extensive tree cover where now there are grasslands (Axelrod 1985) and, presumably, the 100th meridian aridity gradient lay farther west, while during the mid-Holocene, there was extensive dune activity indicating conditions drier than now (Miao et al. 2007) and, likely, an eastward shifted aridity gradient. Now, in addition to continuing natural cycles, rising greenhouse gases from fossil fuel burning are transforming the Earth's climate, and this appears to already be increasing the aridity of the plains. How this will continue to impact the aridity gradient and the 100th meridian, and the implications for the agricultural economy, is the topic of Part II.

**Acknowledgments.** This work was supported by NSF Awards AGS-1243204 and AGS-1401400. A.P.W. was supported by Columbia University's Center for Climate and Life and by the Lamont–Doherty Earth Observatory. We thank Ben Cook, Jason Smerdon, Jack Scheff, Adam Schempp, William DeBuys, Pratigya Polissar, Gidon Eshel, and personnel in the agricultural extension offices for North Dakota, South Dakota, and Kansas for useful conversations; the Lamont Summer Undergraduate Intern program for hosting Nathan Lis and Jamie Feldman during summer 2016; and the reviewers for useful comments and critiques. LDEO Contribution Number 8182-2.

## References

- Allen, R. G., L. S. Pereira, D. Raes, and M. Smith, 1998: Crop evapotranspiration—Guidelines for computing crop water requirements—FAO Irrigation and drainage. Food and Agricultural Organization of the United Nations Irrigation and Drainage Paper 56, 333 pp.
- Axelrod, D. I., 1985: Rise of the grassland biome, central North America. *Bot. Rev.*, **51**, 163–201, <https://doi.org/10.1007/BF02861083>.
- Baltensperger, B. H., 1987: Farm consolidation in the northern and central states of the Great Plains. *Great Plains Quart.*, **7**, 256–265.
- Beerling, D. J., and D. L. Royer, 2011: Convergent Cenozoic CO<sub>2</sub> history. *Nat. Geosci.*, **4**, 418–420, <https://doi.org/10.1038/ngeo1186>.
- Budyko, M. I., and D. H. Miller, 1974: *Climate and Life*. International Geophysics Series, Vol. 18, Academic Press, 508 pp.
- Chiarucci, A., M. R. Araújo, G. Decocq, C. Beierkuhnlein, and J. M. Fernández-Palacios, 2010: The concept of potential natural vegetation: An epitaph? *J. Veg. Sci.*, **21**, 1172–1178, <https://doi.org/10.1111/j.1654-1103.2010.01218.x>.
- Cook, B., J. E. Smerdon, R. Seager, and S. Coats, 2014: Global warming and 21st century drying. *Climate Dyn.*, **43**, 2607–2627, <https://doi.org/10.1007/s00382-014-2075-y>.
- Dai, A., 2011: Characteristics and trends in various forms of the Palmer Drought Severity Index during 1900–2008. *J. Geophys. Res.*, **116**, D12115, <https://doi.org/10.1029/2010JD015541>.
- Daly, C., G. H. Taylor, W. P. Gibson, T. W. Parzybok, G. L. Johnson, and P. Pasteris, 2000: High-quality spatial climate data sets for the United States and beyond. *Trans. Amer. Soc. Agric. Biol. Eng.*, **43**, 1957–1962, <https://doi.org/10.13031/2013.3101>.

- DeBuys, W., Ed., 2001: *Seeing Things Whole: The Essential John Wesley Powell*. Island Press, 320 pp.
- Dee, D., and Coauthors, 2011: The ERA-Interim reanalysis: Configuration and performance of the data assimilation system. *Quart. J. Roy. Meteor. Soc.*, **137**, 553–597, <https://doi.org/10.1002/qj.828>.
- Delworth, T., F. Zeng, A. Rosati, G. A. Vecchi, and A. T. Wittenberg, 2015: A link between the hiatus in global warming and North American drought. *J. Climate*, **28**, 3834–3845, <https://doi.org/10.1175/JCLI-D-14-00616.1>.
- Engle, D. M., B. R. Coppedge, and S. D. Fuhlendorf, 2008: From the Dust Bowl to the green glacier: Human activity and environmental change in Great Plains grasslands. *Western North American Juniperus Communities*, O. W. Van Auken, Ed., Ecological Studies Series, Vol. 196, Springer, 253–271, [https://doi.org/10.1007/978-0-387-34003-6\\_14](https://doi.org/10.1007/978-0-387-34003-6_14).
- Herbert, T. D., K. T. Lawrence, A. Tzanova, L. C. Peterson, R. Caballero-Grill, and C. S. Kelly, 2016: Late Miocene global cooling and the rise of modern ecosystems. *Nat. Geosci.*, **9**, 843–847, <https://doi.org/10.1038/ngeo2813>.
- Higgins, R. W., Y. Chen, and A. V. Douglas, 1999: Interannual variability of the North American warm season precipitation regime. *J. Climate*, **12**, 653–680, [https://doi.org/10.1175/1520-0442\(1999\)012<0653:IVOTNA>2.0.CO;2](https://doi.org/10.1175/1520-0442(1999)012<0653:IVOTNA>2.0.CO;2).
- Homer, C. G., and Coauthors, 2015: Completion of the 2011 National Land Cover Database for the conterminous United States—Representing a decade of land cover change information. *Photogramm. Eng. Remote Sens.*, **81**, 345–354.
- Jacobs, B. F., J. D. Kingston, and L. L. Jacobs, 1999: The origin of grass-dominated ecosystems. *Ann. Mo. Bot. Gard.*, **86**, 590–643, <https://doi.org/10.2307/2666186>.
- Jiang, X., N. Lau, I. M. Held, and J. J. Ploshay, 2007: Mechanisms of the Great Plains low-level jet as simulated in an AGCM. *J. Climate*, **64**, 532–547, <https://doi.org/10.1175/JAS3847.1>.
- Kistler, R., and Coauthors, 2001: The NCEP–NCAR 50-Year Reanalysis: Monthly means CD-ROM and documentation. *Bull. Amer. Meteor. Soc.*, **82**, 247–267, [https://doi.org/10.1175/1520-0477\(2001\)082<0247:TNNYRM>2.3.CO;2](https://doi.org/10.1175/1520-0477(2001)082<0247:TNNYRM>2.3.CO;2).
- Maloney, E. D., and Coauthors, 2014: North American climate in CMIP5 experiments: Part III: Assessment of twenty-first-century projections. *J. Climate*, **27**, 2230–2270, <https://doi.org/10.1175/JCLI-D-13-00273.1>.
- Miao, X., J. A. Mason, J. B. Swinehart, D. B. Loope, P. R. Hanson, R. J. Goble, and X. Liu, 2007: A 10 000 year record of dune activity, dust storms, and severe drought in the central Great Plains. *Geology*, **35**, 119–122, <https://doi.org/10.1130/G23133A.1>.
- Pagani, M., K. H. Freeman, and M. A. Arthur, 1999: Late Miocene atmospheric CO<sub>2</sub> concentrations and the expansion of C<sub>4</sub> grasses. *Science*, **285**, 876–879, <https://doi.org/10.1126/science.285.5429.876>.
- Parish, T. R., and L. D. Oolman, 2010: On the role of sloping terrain in the forcing of the Great Plains low-level jet. *J. Atmos. Sci.*, **67**, 2690–2699, <https://doi.org/10.1175/2010JAS3368.1>.
- Pisani, D., 1992: *To Reclaim a Divided West: Water, Law, and Public Policy, 1848–1902*. University of New Mexico Press, 487 pp.
- Powell, J. W., 1879: Report on the lands of the arid region of the United States, with a more detailed account of the lands of Utah. Government Printing Office, 207 pp.
- , 1890: The irrigable lands of the arid region. *Cent. Mag.*, **39**, 766–776.
- Reif, D. W., and H. B. Bluestein, 2017: A 20-year climatology of nocturnal convection initiation over the central and southern Great Plains during the warm season. *Mon. Wea. Rev.*, **145**, 1615–1639, <https://doi.org/10.1175/MWR-D-16-0340.1>.
- Reisner, M., 1986: *Cadillac Desert: The American West and its Disappearing Water*. Penguin, 582 pp.
- Riley, G. T., M. G. Landin, and L. F. Bosart, 1987: The diurnal variability of precipitation across the central Rockies and adjacent Great Plains. *Mon. Wea. Rev.*, **115**, 1161–1172, [https://doi.org/10.1175/1520-0493\(1987\)115<1161:TVDOPA>2.0.CO;2](https://doi.org/10.1175/1520-0493(1987)115<1161:TVDOPA>2.0.CO;2).

- Rodwell, M. J., and B. J. Hoskins, 2001: Subtropical anticyclones and summer monsoons. *J. Climate*, **14**, 3192–3211, [https://doi.org/10.1175/1520-0442\(2001\)014<3192:SAASM>2.0.CO;2](https://doi.org/10.1175/1520-0442(2001)014<3192:SAASM>2.0.CO;2).
- Scheff, J., and D. M. W. Frierson, 2014: Scaling potential evapotranspiration with greenhouse warming. *J. Climate*, **27**, 1539–1558, <https://doi.org/10.1175/JCLI-D-13-00233.1>.
- Seager, R., and G. A. Vecchi, 2010: Greenhouse warming and the 21st century hydroclimate of southwestern North America. *Proc. Nat. Acad. Sci. USA*, **107**, 21 277–21 282, <https://doi.org/10.1073/pnas.0910856107>.
- , and N. Henderson, 2013: Diagnostic computation of moisture budgets in the ERA-Interim reanalysis with reference to analysis of CMIP-archived atmospheric model data. *J. Climate*, **26**, 7876–7901, <https://doi.org/10.1175/JCLI-D-13-00018.1>.
- , and M. P. Hoerling, 2014: Atmosphere and ocean origins of North American droughts. *J. Climate*, **27**, 4581–4606, <https://doi.org/10.1175/JCLI-D-13-00329.1>.
- , and Coauthors, 2014: Dynamical and thermodynamical causes of large-scale changes in the hydrological cycle over North America in response to global warming. *J. Climate*, **27**, 7921–7948, <https://doi.org/10.1175/JCLI-D-14-00153.1>.
- , A. Hooks, A. P. Williams, B. I. Cook, J. Nakamura, and N. Henderson, 2015: Climatology, variability, and trends in the U.S. vapor pressure deficit, an important fire-related meteorological quantity. *J. Appl. Meteor. Climatol.*, **54**, 1121–1141, <https://doi.org/10.1175/JAMC-D-14-0321.1>.
- , J. R. Feldman, N. Lis, M. Ting, A. P. Williams, J. Nakamura, H. Liu, and N. Henderson, 2018: Whither the 100th meridian? The once and future physical and human geography of America’s arid–humid divide. Part II: The meridian moves east. *Earth Interact.*, **22**, 1–24, <https://doi.org/10.1175/EI-D-17-0012.1>.
- Sheffield, J., E. F. Wood, and M. L. Roderick, 2012: Little change in global drought over the past 60 years. *Nature*, **491**, 435–438, <https://doi.org/10.1038/nature11575>.
- Simon, G. L., 2010: The 100th meridian, ecological boundaries, and the problem of reification. *Soc. Nat. Resour.*, **24**, 95–101, <https://doi.org/10.1080/08941920903284374>.
- Stegner, W., 1954: *Beyond the Hundredth Meridian*. Penguin Books, 496 pp.
- Strömberg, C. A. E., 2011: Evolution of grasses and grassland ecosystems. *Annu. Rev. Earth Planet. Sci.*, **39**, 517–544, <https://doi.org/10.1146/annurev-earth-040809-152402>.
- Ting, M., and H. Wang, 2006: The role of the North American topography on the maintenance of the Great Plains summer low-level jet. *J. Atmos. Sci.*, **63**, 1056–1068, <https://doi.org/10.1175/JAS3664.1>.
- Transeau, E. N., 1905: Forest centers of eastern America. *Amer. Nat.*, **39**, 875–889, <https://doi.org/10.1086/278586>.
- Wallace, J. M., 1975: Diurnal variations in precipitation and thunderstorm frequency over the conterminous United States. *Mon. Wea. Rev.*, **103**, 406–419, [https://doi.org/10.1175/1520-0493\(1975\)103<0406:DVIPAT>2.0.CO;2](https://doi.org/10.1175/1520-0493(1975)103<0406:DVIPAT>2.0.CO;2).
- Webb, W. P., 1931: *The Great Plains*. University of Nebraska Press, 525 pp.
- Xia, Y., and Coauthors, 2012a: Continental-scale water and energy flux analysis and validation for the North American Land Data Assimilation System project phase 2 (NLDAS-2): 1. Intercomparison and application of model products. *J. Geophys. Res.*, **117**, D03109, <https://doi.org/10.1029/2011JD016048>.
- , and Coauthors, 2012b: Continental-scale water and energy flux analysis and validation for North American Land Data Assimilation System project phase 2 (NLDAS-2): 2. Validation of model-simulated streamflow. *J. Geophys. Res.*, **117**, D03110, <https://doi.org/10.1029/2011JD016051>.